Front. Phys. 12(5), 126401 (2017)
DOI 10.1007/s11467-016-0631-0

RESEARCH ARTICLE

Evaporation of a nanodroplet on a rough substrate

Yong-Juan Sun (孙永娟)[1,2], **Tao Huang** (黄韬)[1,2], **Jun-Feng Zhao** (赵俊锋)[1,3], **Yong Chen** (陈勇)[1,3,†]

[1] *Center of Soft Matter Physics and its Applications, Beihang University, Beijing 100191, China*
[2] *Institute of Theoretical Physics, Lanzhou University, Lanzhou 730000, China*
[3] *School of Physics and Nuclear Energy Engineering, Beihang University, Beijing 100191, China*
Corresponding author. E-mail: [†]*ychen@buaa.edu.cn*
Received May 23, 2016; accepted October 8, 2016

The wettability and roughness of a substrate are crucial to the evolution of the contact angle and three-phase contact line in the evaporation of sessile droplets. In this paper, by performing molecular dynamics simulations for droplet evaporation at the nanoscale, we show that the wettability is more important than the roughness. For a smooth substrate, the evaporation behavior of a nanodroplet is similar to that at the macroscopic scale. This similarity is also observed in the case of a rough hydrophilic substrate. However, for a rough hydrophobic substrate, both the constant contact angle and contact line pinning appear in turn during evaporation. This suggests that the roughness of the hydrophobic substrate is useful for the evaporation technique in self-assembly at the nanoscale.

Keywords evaporation, nanodroplet, roughness, wettability

PACS numbers 64.70.F-, 68.03.Fg, 05.70.Ln

1 Introduction

The evaporation of a sessile droplet on a hot surface is of great importance in various practical applications such as coating, inkjet printing, cooling, boiling, washing, and condensation. A significant amount of experimental [1, 2] and theoretical [3, 4] work has been carried out to understand the mechanisms of droplet evaporation. From Young's equation [5], a specific contact angle (CA) can be defined when a liquid droplet is in contact with an ideal flat surface [6]. However, one can almost never get a unique CA in practice since there always exists a contact angle hysteresis (CAH) [7] — the difference between advancing and receding CAs. In addition, the CAH also contributes to the pinning of the three-phase contact line (TPCL) [8, 9], which is the edge of the liquid droplet linking the inside liquid, outside air, and bottom solid substrate.

Surface inhomogeneities are important to TPCL pinning during the droplet evaporation process. In general, there exist two statuses of TPCL dynamics [3, 10]—pinning and depinning. Shina *et al.* claimed that pinning is probably the result of the imperfections of the substrate surface by observing the evaporation of a water droplet on an octadecyltrichlorosilane substrate [2]. Similarly, Grandas *et al.* used the substrate heterogeneity to explain the pinning of a water droplet on polytetrafluoroethylene [11].

The substrate wettability, which is closely linked to its surface properties, should be taken into account when studying the evaporation of a sessile droplet. Many studies, both experimentally and theoretically [1, 12–17], observed three modes of evaporation processes of large droplets [1, 18–22]: (i) the constant-contact-radius (CCR) process [1, 2, 19, 23], in which the TPCL is pinned, but the CA decreases during evaporation ("pinning"); (ii) the constant-contact-angle (CCA) process [1, 19, 23, 24], in which the CA remains constant during evaporation while the TPCL moves ("depinning" or "shrinking"); and (iii) the mixed process [2, 19, 24], where both the CA and the position of the TPCL change with time.

Furuta *et al.* [25] reported that both the nature of the substrate and the droplet size influence the evaporation mechanism in their experimental study of water droplets (about 0.1 mm and 1 mm in diameter) evaporating from hydrophilic and hydrophobic substrates. However, it is still not clear whether nanodroplet evaporation has the same above-mentioned properties as normal droplets. Usually, the validity of the macroscopic evaporation results becomes questionable in nanoscopic domains [1, 26]. In this study, we employed molecular dynamics (MD) simulations to study the effects of the

wettability and roughness of the substrate on the evaporation of sessile nanodroplets. It was found that the wettability of the substrate is more important than the roughness of the substrate during temperature-raising evaporation. Otherwise, the roughness of the substrate induces more complicated evaporation modes, especially in the case of a hydrophobic substrate.

In Section 2, we describe the simulation configuration and detailed initial setup. Moreover, we introduce the definition of roughness. Next, in Section 3, we present the simulation results including the time evolution of the temperature, droplet size, liquid density, sphericity, CA, and contact radius (CR) for the combination of the roughness and wettability of the substrate. Furthermore, the evaporation modes for different substrates with the above-mentioned combination are studied. Finally, in Section 4, we conclude with a discussion of our results.

2 Model and methods

We set up the model consisting of a liquid nanodroplet surrounded by its gas phase and a solid substrate. All atoms are modeled by Lennard–Jones atoms with the nonbonded 12-6 potential

$$U_{ab}(r_{ij}) = 4\epsilon_{ab}\left[\left(\frac{\sigma_{ab}}{r_{ij}}\right)^{12} - \left(\frac{\sigma_{ab}}{r_{ij}}\right)^{6}\right], \quad (1)$$

where r_{ij} is the distance between atoms i and j, σ_{ab} is the collision diameter at which the potential is zero, and ϵ_{ab} is the depth of the potential well. The subscripts a and b denote different atom types, which can be substituted by l (liquid) or s (solid). In our simulations, the parameters $\sigma_{ll} = 0.3405$ nm and $\epsilon_{ll} = 0.992$ kJ/mol are used for the liquid atoms (argon), and $\sigma_{ss} = 0.4085$ nm and $\epsilon_{ss} = 9.92$ kJ/mol are for the solid substrate atoms. The mass of a solid atom is 10 times that of a liquid atom. All quantities are expressed in reduced units based on the parameters σ_{ll}, ϵ_{ll}, and $m_l = (6.63 \times 10^{-26}$ kg) of a liquid atom. The temperature unit $T^* = k_B T/\epsilon_{ll} = 1$ corresponds to 119.8 K. The time unit $\tau = \sqrt{m_l \sigma_{ll}^2/\epsilon_{ll}} = 1$ corresponds to 5 ps. Moreover, the value of $\sigma_{ls}^* = 1.1$ is used.

Note that the energy parameter ϵ_{ls}^* reflects the chemical nature of the substrates. Thus, $\epsilon_{ls}^* < 0.5$ means a hydrophobic substrate with a CA of $\theta > \pi/2$, and $\epsilon_{ls}^* > 0.5$ corresponds to a hydrophilic substrate with $\theta < \pi/2$ [24]. In our simulations, ϵ_{ls}^* is set as 0.4 or 0.7, respectively corresponding to the hydrophobic and hydrophilic substrates. We name the hydrophobic system with a smooth (rough) substrate sE4 (rE4) when $\epsilon_{ls}^* = 0.4$. Similarly, sE7 (rE7) denotes the hydrophilic system containing a smooth (rough) substrate with $\epsilon_{ls}^* = 0.7$.

A quantitative definition of the roughness factor is the following form [27]:

$$r = s_a/s_g, \quad (2)$$

where the s_a is the total actual area of an interface, and the s_g is the geometric surface measured in the plane of the interface, where perfect smoothness is an acceptable assumption. For a liquid–liquid or liquid–gas interface, s_a and s_g are identical, but at the surface of any real solid, s_a will be greater than s_g because of the surface roughness [27]. When $r = 1$, the substrate is smooth, and $r > 1$ corresponds to a rough substrate. In our simulations, $r = 1$ for a smooth substrate and 2.901 43 for rough substrate. The geometric surface shape is described by the spatial function $z(x, y) = A \cos x \cos y$, where z is the vertical axis, (x, y) represents the horizontal plane, and A denotes the amplitude. Figure 1 shows a side view of the substrate.

The total number of argon atoms for the liquid and gas phases is set as 27 000. These atoms are initially distributed in a cubic box with a liquid density. The solid substrate is modeled with a face-centered cubic (FCC) lattice. The total numbers of solid atoms for the smooth and rough systems are 23 040 and 36 864, respectively. The substrate is placed at the bottom of the simulation box (31.104 nm in the x and y directions and 50 nm in the z direction), and initially, the liquid sphere is on the substrate.

All MD simulations presented in this work are carried out in the NVT ensemble (i.e., the number of atoms N, the volume V, and the temperature T of the system are kept constant), in which the Berendsen thermostat with a coupling time of $0.25\,\tau$ is chosen to control the temperature [28]. Note that the thermostat is only applied to the substrate atoms during the heating process. The periodic boundary condition is enforced by using the

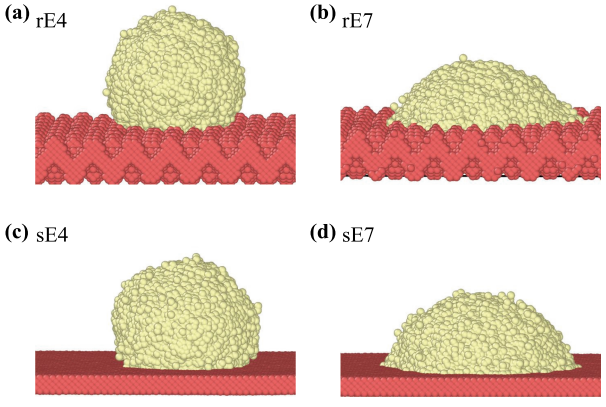

Fig. 1 The snapshots of nanodroplets upon solid substrates at time $15\,000\,\tau$ in our simulations. The upper panels are of rough substrate ($r = 2.901\,43$) and the lower is smooth ($r = 1.0$). The substrates in left panels are hydrophobic (ϵ_{ls}^*=0.4) and the right is hydrophilic (ϵ_{ls}^*=0.7).

parallelized code of LAMMPS [29]. The time step and cut-off distance are $0.0025\,\tau$ (5 fs) and $3.0\,\sigma_{ll}$ (1.023 nm), respectively.

The whole simulation process undergoes two stages. At first, the systems for all scenarios (rE4, sE4, rE7, and sE7) relax to their equilibrium configurations at the temperature $T^* = 0.67$, where a droplet is surrounded by its gas phase. Then, the temperature of the solid substrate is reset to 0.83 at the time $15000\,\tau$. The whole evaporation process in this part consists of two stages, temperature-raising evaporation and the subsequent constant-temperature evaporation with a nanodroplet temperature of 0.83. Figure 1 shows the spherical droplets on the smooth/rough solid substrates with different hydrophilicities.

We use the cluster analysis method to distinguish the liquid phase from the gas phase. Two atoms are considered to be in the same cluster if the distance between them is smaller than $1.5\,\sigma_{ll}$. In order to calculate the liquid density in the droplet, the nanodroplet is divided into 90 vertical slices with a width of $1.2\,\sigma_{ll}$ around the central vertical z-axis. Then, we can calculate the CR and CA by fitting the contour curves of the liquid density with a circular arc [4].

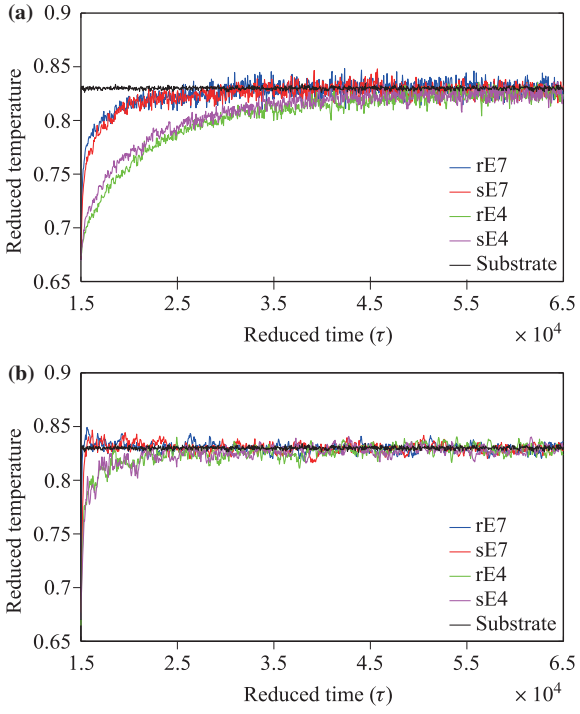

Fig. 2 Time evolution of the temperatures of **(a)** nanodroplet and **(b)** vapor. Here, the temperature of solid substrate denoted by black solid line is fixed at $T^* = 0.83$.

3 Results and discussion

3.1 Temperature

Figure 2 plots the time evolution of the temperatures in the evaporating processes. It is clear that the evaporation of a nanodroplet undergoes two stages as mentioned above, temperature-raising evaporation and the subsequent constant-temperature evaporation at a substrate temperature equal to 0.83 [see Fig. 2(a)]. Moreover, the period of the temperature up to the stable temperature of 0.83 for the vapor is shorter than that for the nanodroplets. Qualitatively, this is because the vapor has fewer particles but a larger contact area with the substrate than the nanodroplet. It is much more important that the molecule should have a larger kinetic energy to evaporate with a higher probability from the liquid–vapor interfacial region.

Note that, in the temperature-raising stage, the temperature increase of the hydrophilic cases (E7) is much quicker than that of the hydrophobic cases (E4) since the stronger liquid–solid interaction in E7 results in more efficient heat transfer. For the same hydrophilicity (E7), the temperature of the droplets upon the rough substrate increases a little faster than that upon the smooth substrates because of the larger contact areas between the liquid droplet and the solid substrate. Contrarily, in the case of the hydrophobic substrates (E4), the rough substrate makes the temperature of droplets increase a little slower. The higher wettability and roughness of the substrate results in much more efficient heat transfer. In comparison, the wettability of substrate is more crucial than the surface roughness to the heat transfer at the nanoscale. Besides, the roughness of the substrate does not have any noticeable effect on the temperature increase of the vapor [see Fig. 2(b)].

3.2 Nanodroplet size and liquid density

The initial number of argon atoms in the simulation box is 27 000. When the systems reach equilibrium at $T^* = 0.67$, steady droplets are formed with numbers of atoms of about 20 236, 22 692, 22 842, and 22 917 for the rE7, sE7, rE4, and sE4 scenarios, respectively. Figure 3 shows the numbers of atoms inside the droplets as a function of the time during evaporation after the temperature of the substrate was suddenly increased to 0.83 at time $15\,000\,\tau$. In all cases, the droplet size decreases quickly in the stage of temperature-raising evaporation and then reaches a steady size in the constant-temperature evaporation stage. The final steady size of the droplet upon the hydrophilic substrate is clearly smaller than that upon the hydrophobic one. Similarly, in the case of the hydrophilic substrates (E7), the rough surface increases the

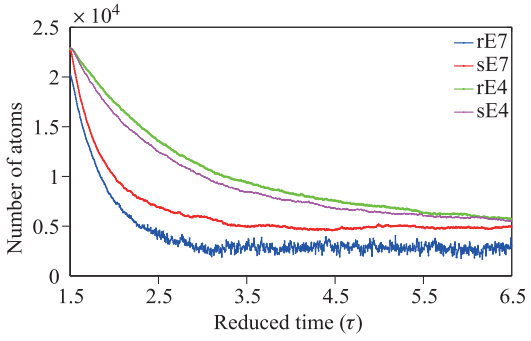

Fig. 3 The atom numbers inside the nanodroplets as a function of time during the evaporation upon the substrate $T^* = 0.83$.

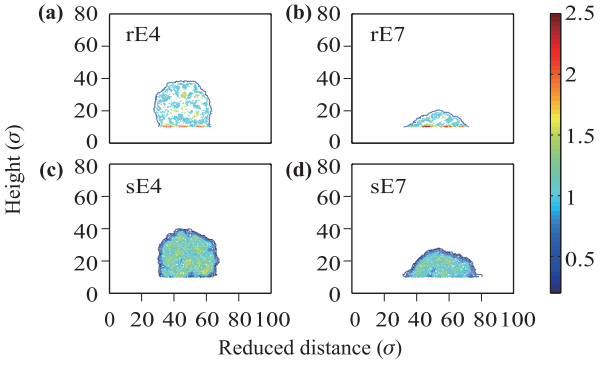

Fig. 4 The distributions of liquid density in nanodroplets at time 20 000 τ in our simulations.

shrinking speed of the droplet size in the first stage, and the system will reach a lower final steady size. For the E4 scenario (hydrophobic substrates), the rougher surface slightly lowers the shrinking speed.

Figure 4 presents side views of the average liquid density in the nanodroplets at time 20 000 τ in the temperature-raising stage. Here, we set a small box with 1.2 σ in the x direction and 2 σ in the y and z directions and then use the box-shift technique to calculate the average local particle number density of the nanodroplet. In all cases, the shape of the droplet still maintains an approximate spherical cap upon the heated substrate, and we will quantitatively discuss again in the following context. It is clear that there is a low-density outer layer near the liquid–vapor interface. For the scenarios with a smooth substrate, the liquid density inside the droplet is fairly homogeneous but is inhomogeneous for rough substrates. Moreover, we observe that there are some small areas upon the rough surface with a higher density [Figs. 4(a) and (b)]. They are thought to result from local stable molecules trapped by the valleys on the rough substrate.

3.3 Contact angle, contact radius, and sphericity

In fact, the shape of a droplet is not exactly spherical, and there exists a slight or even strong (at a high temperature) deformation during evaporation. From the example shown in Fig. 5(a), 90 samples of the CA are calculated for the side-view arcs of the droplet surface at time 15 000 τ ($T^* = 0.67$) in the case of the sE4 scenario. It shows that the average value 117.46° is large, but in fact, the relative deviation is very small (0.98%). Therefore, in the following calculation of the CA and CR, we average over 90 samples along the TPCL with an interval of 2° to reduce the effect of droplet deformation.

A quantitative parameter of the deformation of the droplet surface, the droplet sphericity S, is defined as

$$S = R_{small}/R_{large}, \tag{3}$$

where R_{small} and R_{large} are the separate averages of 45 smaller spherical radii and of the remaining 45 larger radii, respectively. If S is equal to 1, the droplet is perfectly spherical; otherwise, it is deformed [30]. Moreover, the cases with $S < 0.5$ cannot be considered as a spherical cap any more.

Figure 5(b) shows that, after a slight decrease in the temperature-raising stage, all of the sphericities converge

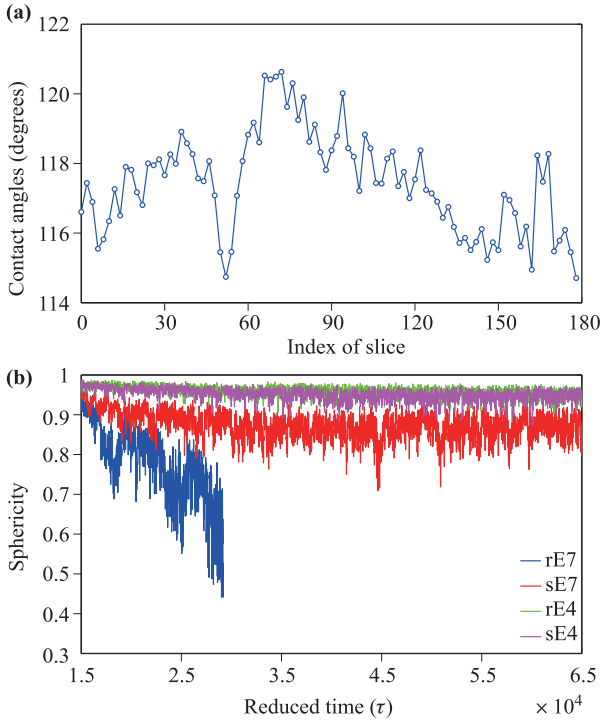

Fig. 5 **(a)** The distribution of contact angles along the TPCL of a droplet from sE4 system at time 15 000 τ. The average CA is 117.46° and the relative deviation is 0.98%. **(b)** Time evolution of the sphericity of the droplets for all four scenarios.

to their steady values, about 0.952 for rE4, 0.935 for sE4, and 0.888 for sE7. However, the sphericity for rE7 decreases quickly to a very small value because of the higher mass flux. A smaller value of the sphericity (normally $S < 0.5$) means that the droplet cannot really be considered as a spherical cap. The sphericity for all four systems appears as an obvious fluctuation during the whole evaporation process. The hydrophilic systems (E7) always exhibit stronger fluctuation of the sphericities, corresponding to a larger deformation of the nanodroplet shape. It is qualitatively conjectured that the hydrophilicity enhances the mass flux inside the droplet, then leads to a higher evaporation rate, and results in stronger deformation of the liquid–vapor interface.

Interestingly, in the case of the hydrophilic scenario (E7), S for the rough substrate (rE7) is smaller than that for the smooth case (sE7). However, for the hydrophobic systems (E4), the sphericity has much different behavior in that S for rE4 is slightly larger than that for sE4 [See Fig. 5(b)]. Again, this is because the rough substrate enhances the mass flux in hydrophilic systems but suppresses it in hydrophobic systems.

Figure 6 plots the time evolutions of the CA and CR for all four scenarios to study the evaporation modes, as mentioned above. In the case of rE4 [Fig. 6(a)], initially, the evaporation follows the CCA mode (a constant CA of 131.06 and a linearly shrinking CR with a slope of -1.95×10^{-4}), and after time $32\,500\,\tau$, undergoes a sudden jump in the CA, and then changes to the CCR mode (a linearly decreasing CA with a slope of -1.34×10^{-4} and a constant CR of 8.63). Here, the unusual jump in the CA probably results from the deformation of a droplet with a smaller size to fit with the stronger hydrophobic substrate. For the rE7 scenario [Fig. 6(b)], both the CA and CR always linearly decrease throughout the whole evaporation process with slopes of -0.0013 and -0.0012, respectively. This is the so-called mixed mode. In the cases of the smooth substrate (sE4 and sE7), as shown in Figs. 6(c) and (d), both droplets exhibit evaporation in the CCA mode (the CA is 121.66 for sE4 and 76.38 for sE7). However, the CRs no longer linearly decrease and are subjected to an exponential decay, $9.81 + 19.99\exp(-6.97 \times 10^{-5}t)$ and $15.08 + 107.43\exp(-1.61 \times 10^{-4}t)$ for sE4 and sE7, respectively. Here, t is the reduced time.

These evaporation properties at the nanoscale are quite different from the experimental observations at the macroscopic ($> 100\,\mu$m in diameter) and mesoscopic (1–100 μm in diameter) scales, at which the CCA or CCR modes are usually observed [30]. The pinning phenomena during droplet evaporation are usually assumed to be result of the heterogeneities of the substrates [2, 11, 16]. However, in our simulations of nanodroplet evaporation for rough substrates (rE4 and rE7), the TPCL shrinks in the temperature-raising stage, and the CR always keeps shrinking for rE7.

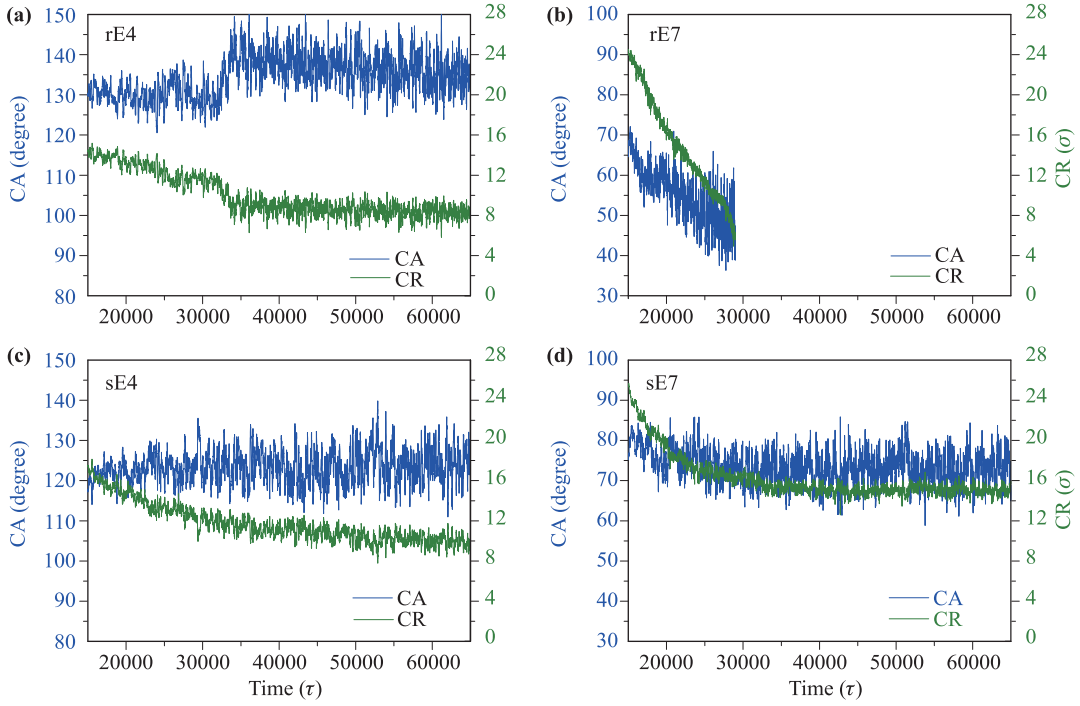

Fig. 6 Time evolutions of CA and CR for **(a)** rE4, **(b)** rE7, **(c)** sE4, and **(d)** sE7 systems. Note that the data series in panel *b* is much shorter than others because of no droplet upon the substrate due to quick evaporation.

4 Summary

In this paper, we performed MD simulations to study the evaporation of nanodroplets upon heated smooth/rough hydrophilic/hydrophobic substrates. By calculating the time evolutions of several parameter sets during nanodroplet evaporation (the temperature, sphericity, CA, and CR), it is found that the wettability of the substrate plays a more important role than the roughness of the substrate. Basically, the rough substrate enhances evaporation in the case of a hydrophilic substrate but suppresses it for a hydrophobic substrate.

The whole evaporation process of droplets at the nanoscale upon smooth hydrophobic and hydrophilic substrates appears to be evaporation in the CCA mode, except the very short early time. However, for the rough substrate, the evaporation properties of the nanodroplets are different from the CCA or CCR for macroscopic/mesoscopic evaporation. When the rough substrate is hydrophilic, we observed a mixed evaporation mode [Fig. 6(b)]. The evaporation behaviors of a nanodroplet upon a rough hydrophobic substrate are complicated [Fig. 6(a)]. The simulation results reveal that its evaporation is composed of the CCA and CCR. Especially, there exists a jump in the CA between the two modes in the temperature-raising stage. In principle, the temperature increase reduces the CA during droplet evaporation [30]. Here, this anomalous jump in the CA is partly due to the dependence of the CA on the contact-line curvature and its sensitivity to the substrate roughness [31].

Acknowledgements This work was supported by the National Natural Science Foundation of China under Grant No. 11275084 and Grant No. 21434001.

References

1. D. S. Golovko, H. J. Butt, and E. Bonaccurso, Transition in the evaporation kinetics of water microdrops on hydrophilic surfaces, *Langmuir* 25(1), 75 (2009)
2. D. H. Shina, S. H. Lee, J. Y. Jung, and J. Y. Yoo, Evaporating characteristics of sessile droplet on hydrophobic and hydrophilic surfaces, *Microelectron. Eng.* 86(4–6), 1350 (2009)
3. T. A. H. Nguyen, A. V. Nguyen, M. A. Hampton, Z. P. Xu, L. B. Huang, and V. Rudolph, Theoretical and experimental analysis of droplet evaporation on solid surfaces, *Chem. Eng. Sci.* 69(1), 522 (2012)
4. J. Zhang, F. Leroy, and F. Müller-Plathe, Influence of contact-line curvature on the evaporation of nanodroplets from solid substrates, *Phys. Rev. Lett.* 113(4), 046101 (2014)
5. F. C. Wang and Y. P. Zhao, Contact angle hysteresis at the nanoscale: A molecular dynamics simulation study, *Colloid Polym. Sci.* 291(2), 307 (2013)
6. T. Young, An essay on the cohesion of fluids, *Philos. Trans. R. Soc. Lond. B* 95(0), 65 (1805)
7. P. G. de Gennes, Wetting: Statics and dynamics, *Rev. Mod. Phys.* 57(3), 827 (1985)
8. C. W. Extrand and Y. Kumagai, An experimental study of contact angle hysteresis, *J. Colloid Interface Sci.* 191(2), 378 (1997)
9. C. W. Extrand, A thermodynamic model for contact angle hysteresis, *J. Colloid Interface Sci.* 207(1), 11 (1998)
10. P. G. Pittoni, C. C. Chang, T. S. Yu, and S. Y. Lin, Evaporation of water drops on polymer surfaces: Pinning, depinning and dynamics of the triple line, *Colloids Surf. A* 432, 89 (2013)
11. L. Grandas, C. Reynard, R. Santini, and L. Tadrist, Experimental study of the evaporation of a sessile drop on a heat wall: Wetting influence, *Int. J. Therm. Sci.* 44(2), 137 (2005)
12. H. Huand and R. G. Larson, Evaporation of a sessile droplet on a substrate, *J. Phys. Chem. B* 106(6), 1334 (2002)
13. X. Shen, C. M. Ho, and T. S. Wong, Minimal size of coffee ring structure, *J. Phys. Chem. B* 114(16), 5269 (2010)
14. B. J. Fischer, Particle convection in an evaporating colloidal droplet, *Langmuir* 18(1), 60 (2002)
15. H. M. Gorr, J. M. Zueger, and J. A. Barnard, Lysozyme pattern formation in evaporating drops, *Langmuir* 28(9), 4039 (2012)
16. D. Orejon, K. Sefiane, and M. E. R. Shanahan, Stick-slip of evaporating droplets: Substrate hydrophobicity and nanoparticle concentration, *Langmuir* 27(21), 12834 (2011)
17. S. Maheshwari, L. Zhang, Y. Zhu, and H. C. Chang, Coupling between precipitation and contact-line dynamics: Multiring stains and stick-slip motion, *Phys. Rev. Lett.* 100(4), 044503 (2008)
18. T. Furuta, A. Nakajima, M. Sakai, T. Isobe, Y. Kameshima, and K. Okada, Evaporation and sliding of water droplets on fluoroalkylsilane coatings with nanoscale roughness, *Langmuir* 25(10), 5417 (2009)
19. J. H. Kim, S. I. Ahn, J. H. Kim, and W. C. Zin, Evaporation of water droplets on polymer surfaces, *Langmuir* 23(11), 6163 (2007)
20. G. McHale, S. M. Rowan, M. I. Newton, and M. K. Banerjee, Evaporation and the wetting of a low-energy solid surface, *J. Phys. Chem. B* 102(11), 1964 (1998)
21. G. Li, S. M. Flores, C. Vavilala, M. Schmittel, and K. Graf, Evaporation dynamics of microdroplets on self-assembled monolayers of dialkyl disulfides, *Langmuir* 25(23), 13438 (2009)

22. K. R. Khedir, G. K. Kannarpady, H. Ishihara, J. Woo, S. Trigwell, C. Ryerson, and A. S. Biris, Advanced studies of water evaporation kinetics over teflon-coated tungsten nanorod surfaces with variable hydrophobicity and morphology, *J. Phys. Chem. C* 115(28), 13804 (2011)

23. K. S. Birdi and D. T. Vu, Wettability and the evaporation rates of fluids from solid surfaces, *J. Adhes. Sci. Technol.* 7(6), 485 (1993)

24. Y. Liu and X. Zhang, Evaporation dynamics of nanodroplets and their anomalous stability on rough substrates, *Phys. Rev. E* 88(1), 012404 (2013)

25. T. Furuta, M. Sakai, T. Isobe, and A. Nakajima, Evaporation behavior of microliter- and sub-nanoliter-scale water droplets on two different fluoroalkylsilane coatings, *Langmuir* 25(20), 11998 (2009)

26. R. V. Sedev, J. G. Petrov, and A. W. Neumann, Effect of swelling of a polymer surface on advancing and receding contact angles, *J. Colloid Interface Sci.* 180(1), 36 (1996)

27. R. N. Wenzel, Resistance of solid surfaces to wetting by water, *Ind. Eng. Chem.* 28(8), 988 (1936)

28. H. J. C. Berendsen, J. P. M. Postma, W. F. van Gunsteren, A. DiNola, and J. R. Haak, Molecular dynamics with coupling to an external bath, *J. Chem. Phys.* 81(8), 3684 (1984)

29. S. Plimpton, Fast parallel algorithms for short-range molecular dynamics, *J. Comput. Phys.* 117(1), 1 (1995)

30. J. Zhang, F. Leroy, and F. Müller-Plathe, Evaporation of nanodroplets on heated substrates: A molecular dynamics simulation study, *Langmuir* 29(31), 9770 (2013)

31. A. Checco, P. Guenoun, and J. Daillant, Nonlinear dependence of the contact angle of nanodroplets on contact line curvature, *Phys. Rev. Lett.* 91(18), 186101 (2003)